Dillon Stacey R. (Orcid ID: 0000-0001-8758-3795)

Running Head: DUAL ICOS/CD28 BLOCKADE IN ARTHRITIS MODELS

Dual Blockade of ICOS and CD28 with Acazicolcept (ALPN-101) Reveals Non-Redundant Roles of T Cell Co-Stimulation Pathways in Inflammatory Arthritis

Stacey R. Dillon, Lawrence S. Evans, Katherine E. Lewis, Susan Debrot, Tiffany C. Blair, Sherri Mudri, Kayla Kleist[1], Steven D. Levin[1], Janhavi G. Bhandari, Logan Garrett, Martin F. Wolfson, Pamela M. Holland, Mark W. Rixon, and Stanford L. Peng

Stacey R. Dillon, PhD, Lawrence S. Evans, BS, Katherine E. Lewis, PhD, Susan Debrot, BS, Tiffany C. Blair, PhD, Sherri Mudri, BS, Kayla Kleist, MS, Steven D. Levin, PhD, Janhavi G. Bhandari, MS, Logan Garrett, BS, Martin F. Wolfson, BS, Pamela M. Holland, PhD, Mark W. Rixon, PhD, and Stanford L. Peng, MD, PhD: Alpine Immune Sciences, Seattle, WA

All authors are current or former[1] employees of, and own stock or stock options in, Alpine Immune Sciences, Inc. Seattle, WA, USA

Address correspondence to Stacey Dillon, Ph.D., 188 E. Blaine St., Suite 200, Seattle, WA 98102. Email: Stacey.Dillon@alpineimmunesciences.com; office phone: 206-788-4545.

This article has been accepted for publication and undergone full peer review but has not been through the copyediting, typesetting, pagination and proofreading process which may lead to differences between this version and the Version of Record. Please cite this article as doi: 10.1002/art.42484

ABSTRACT

Objective

CD28 and inducible T cell costimulator (ICOS) appear to play non-redundant roles in T cell activation and adaptive immunity. Acazicolcept (ALPN-101), an Fc fusion protein of a human variant ICOS Ligand (ICOSL) domain designed to inhibit both CD28 and ICOS costimulation, was characterized for therapeutic potential in inflammatory arthritis in vitro and in vivo.

Methods

Acazicolcept was compared to inhibitors of either the ICOS or CD28 pathways (abatacept and belatacept [CTLA-4-Ig], prezalumab [anti-ICOSL mAb]) in vitro, in receptor binding and signaling assays, and in a collagen-induced arthritis (CIA) model. Acazicolcept was also compared in cytokine and/or gene expression assays of PBMC from healthy donors or rheumatoid arthritis (RA) or psoriatic arthritis (PsA) patients, stimulated with artificial antigen presenting cells (aAPC) expressing CD28 and ICOS ligands.

Results

Acazicolcept bound CD28 and ICOS, prevented ligand binding, and inhibited human T cell functional interactions, matching or exceeding the activity of CD28 or ICOS costimulatory single pathway inhibitors tested individually or in combination. Acazicolcept administration reduced disease in the CIA model significantly and more potently than abatacept. Acazicolcept also inhibited

pro-inflammatory cytokine production from stimulated PBMC in co-cultures with aAPC and demonstrated unique impacts on gene expression distinct from those induced by abatacept, prezalumab, or a combination of both.

Conclusion

Both CD28 and ICOS signaling play critical roles in inflammatory arthritis. Therapeutic agents such as acazicolcept that co-inhibit both ICOS and CD28 signaling may mitigate inflammation and/or disease progression in RA and PsA more effectively than inhibitors of either pathway alone.

INTRODUCTION

Dysregulation of T cell activation and adaptive immunity is a significant contributor to autoimmune diseases including rheumatoid arthritis (RA) and psoriatic arthritis (PsA) (1, 2). Sustained T cell activation through the T cell receptor (TCR) requires additional signaling from co-stimulatory receptors, and blockade of co-stimulatory pathways has emerged as a promising tool for the treatment of autoimmune diseases (3). Immunoglobulin superfamily (IgSF) proteins are attractive therapeutic targets in immune disorders. Two important IgSF co-stimulatory molecules are cluster of differentiation 28 (CD28) and inducible T cell costimulator (ICOS) (4). Absence or blockade of either CD28 or ICOS leads to poor or incomplete T cell activation, providing the rationale for their inhibition in the treatment of autoimmune/inflammatory disorders such as

RA, juvenile idiopathic arthritis (JIA), PsA, graft versus host disease (GVHD), inflammatory bowel disease (IBD), and Sjögren's syndrome (5-9).

CD28 is activated by engagement of the ligands CD80 and CD86 expressed on antigen presenting cells (APC). CD28 stimulation is critical for activation of naïve and memory CD4+ T cells, and enhances IL-2 production, cell cycle progression, and T cell survival. Another IgSF member, CTLA-4, also engages CD80 and CD86 but plays an inhibitory role in T cell activation, thus acting as a counterbalance to CD28 costimulation.

Abatacept is an FDA-approved drug that comprises the extracellular domain of human CTLA-4 fused to IgG1 Fc and mediates immunosuppressive effects by binding CD80 and CD86 and blocking their interactions with CD28/CTLA-4. The second-generation CTLA-4-Ig belatacept differs from abatacept by two amino acid substitutions in the CTLA-4 domain that confer greater binding avidity to CD80 and CD86 (10). Abatacept is approved for RA (11), PsA (12), and juvenile idiopathic arthritis (5, 13) and prevention of acute GVHD (6), while belatacept is indicated for prevention of renal allograft rejection (14). However, treatment with CTLA-4-Ig therapies does not result in complete remission and/or suppression of T cell-mediated inflammatory activity in most patients (15, 16), suggesting involvement of additional pathogenic pathways.

As the most closely related IgSF to CD28, ICOS may contribute to CD28-independent costimulation. Like CD28, ICOS provides a positive T cell costimulatory signal and has been implicated in the induction and regulation of Th1, Th2, and Th17 immunity (17, 18). In addition to directing effector T cell differentiation, ICOS has also been linked with the induction of T cell-dependent antibody responses and with germinal center (GC) reactions (17, 19). ICOS costimulation, therefore, plays a complex role in dictating the course of adaptive immunity, and ICOS deficiency leads to defective humoral responses in mice and humans (20). Unlike CD28, ICOS is not constitutively expressed on naïve T cells but is rapidly upregulated after TCR engagement and may represent a key pathogenic pathway unaddressed by CD28 antagonism. ICOS upregulation correlates with disease activity in several inflammatory diseases, and in preliminary studies prezalumab (AMG 557/MEDI5872), a blocking human monoclonal antibody (mAb) against ICOSL, demonstrated potential benefit in lupus arthritis (21-26) and Sjögren's syndrome (27). However, no ICOS pathway antagonists are currently approved for therapeutic use.

Despite structural similarities and engagement of common downstream pathways, it is clear that ICOS and CD28 play non-redundant roles in T cell activation (18), which may in part explain the disappointing results observed with therapeutic agents targeting either of these pathways separately. In preclinical models, combined blockade and/or deficiency of both CD28 and ICOS is advantageous

for islet allograft survival (28), inflammatory bowel disease (IBD) (7), delayed-type hypersensitivity (29), GVHD (30, 31), and systemic sclerosis (32).

A platform utilizing directed evolution of IgSF proteins to produce variant immunoglobulin domains (vIgDs) with increased affinity for cognate counter-structure ligands has been described (32). Using this engineering platform, we derived ICOSL domains with enhanced binding to ICOS and increased high-affinity binding to CD28. The therapeutic candidate acazicolcept (ALPN-101; ICOSL vIgD-Fc) is a selected dimer of an engineered ICOSL vIgD domain fused to an IgG1 Fc lacking effector function (Fig 1A), and was designed to potently inhibit CD28 and ICOS costimulation (Figure 1B) (33). Acazicolcept demonstrates promising efficacy in multiple inflammatory models including acute GVHD (31) and systemic sclerosis (32). Because the CD28 pathway has been clinically validated in RA and PsA, we examined the potential therapeutic advantage of dual CD28/ICOS inhibition in inflammatory arthritis.

MATERIALS AND METHODS

Acazicolcept and comparators

Acazicolcept is a dimer of a ICOSL vIgD domain fused to an IgG1 Fc lacking effector function. The generation of acazicolcept was previously described (31, 33). See the Supplementary Methods for details.

Binding of acazicolcept to CD28 and ICOS and inhibition of ligand binding

To measure binding to CD28 and ICOS, acazicolcept or comparators were titrated and incubated with Chinese hamster ovary (CHO) cells transfected with human CD28 or ICOS, detected with anti-human IgG-PE, and measured by flow cytometry. See the Supplementary Methods for full details.

Costimulation assay for functional characterization of acazicolcept

Full details of the costimulation assay are provided in Supplementary Methods. Briefly, artificial antigen presenting cells (aAPC) were generated by transducing K562 cells with lentivirus to express cell surface anti-human CD3 single chain variable fragment and full-length human CD80, and/or CD86, and/or ICOSL. Cell surface transgene expression was confirmed by flow cytometry.

Mouse collagen-induced arthritis model

Details on the mouse CIA model and endpoint analyses are provided in Supplementary Methods. Briefly, DBA/1 mice (n=15/group) were immunized with bovine collagen in Complete Freund's Adjuvant to induce arthritis and then treated with acazicolcept or comparators. Severity of disease was assessed over time.

Human PBMC stimulation and cytokine assays

PBMC from RA or PsA patients and healthy donors were stimulated with aAPC (K562/OKT3/CD80/CD86/ICOSL) for 48 hours in the presence of 100 nM of each test article or 100 nM each for the abatacept+prezalumab combination. See the Supplementary Methods for full details.

Gene expression analysis

Full details of the gene expression analysis are provided in Supplementary Methods. Briefly, total RNA (0.5 ng) was added to lysis buffer from the SMART-Seq v4 Ultra Low Input RNA Kit for Sequencing (Takara) and subjected to RT-PCR to generate full-length amplified cDNA. Sequencing libraries were constructed using the NexteraXT DNA sample preparation kit (Illumina) to generate Illumina-compatible barcoded libraries.

RESULTS

Acazicolcept binds CD28 and ICOS and prevents ligand binding

Acazicolcept bound both CD28 and ICOS, with greater binding to ICOS compared to a WT ICOSL Fc fusion (Figure 1C). IC_{50} values for inhibition of ligand binding (Figure 1D) confirmed that acazicolcept inhibited CD80 and CD86 binding to CD28 and ICOSL binding to ICOS more effectively than abatacept, belatacept, or WT ICOSL-Fc.

Functional blockade of CD28 costimulation by acazicolcept was demonstrated by suppression of the ability of artificial APCs (aAPC) expressing OKT3 (anti-CD3) and human CD86 to stimulate Jurkat/IL-2 cells expressing endogenous CD28 and co-expressing luciferase driven from an IL-2 promoter. Acazicolcept showed superior blockade of CD28 costimulation compared with either abatacept or belatacept (Figure 1E). In a parallel test of ICOS co-stimulation, acazicolcept inhibited the ability of aAPC expressing OKT3 and human ICOSL to stimulate ICOS on Jurkat/IL-2 cells transduced with $ICOS_{ECD}/CD28_{ICD}$, showing similar efficacy to prezalumab (Figure 1E).

Together, these data demonstrate that acazicolcept binds both human CD28 and ICOS and inhibits ligand-mediated costimulation. Acazicolcept inhibits the CD28 pathway more effectively than abatacept or belatacept and inhibits the ICOS pathway comparably to the monoclonal antibody prezalumab.

Acazicolcept displays enhanced efficacy over abatacept in a mouse collagen-induced arthritis model

Previous studies confirmed that acazicolcept binds mouse ICOS, CD28, and CTLA-4, with EC_{50} values roughly twice those calculated for the human receptors (31). As abatacept is an approved therapeutic for RA and also binds sufficiently to mouse CD80 and CD86 (34, 35), it was compared to acazicolcept in the mouse CIA model (36, 37).

For dosing in the CIA model (described in Supplementary Figure 1A), treatment was initiated on the day of the collagen boost (Study Day 18). Treatment of mice with five doses of acazicolcept administered every 3 days significantly delayed onset and severity of arthritic disease compared to mice treated with Dulbecco's phosphate buffered saline (DPBS) or molar matched amounts of Fc control or abatacept. Overall, acazicolcept-treated mice maintained or gained body weight over the course of the study, while mice in all other groups lost weight (p=0.0003 and p=0.0061 for % of initial BW for acazicolcept compared with DPBS or Fc control groups, respectively) (Figure 2A). Mean CIA paw scores measured over time were significantly lower in the acazicolcept versus the DPBS or Fc control groups (p<0.0001), and versus the abatacept group (p=0.0016) (Figure 2B), although abatacept conferred some protection from disease severity compared with DPBS (p=0.0006) and Fc control-treated mice (p=0.0172). The final median paw score (Day 34) for the acazicolcept group was 3.0 (interquartile range of 0 – 4.0) out of a maximum possible score of 16, which was significantly lower than that of the DPBS (13.5 [10.0–16.0]; p<0.0001), Fc control (13.0 [12.0–16.0.]; p<0.0001), and abatacept (9.0 [5.25–13.0]; p<0.048) groups (Supplementary Figure 1B). Abatacept showed no significant improvement over DPBS or Fc control for final CIA score (p=0.079 and p=0.138, respectively) due to the high degree of inter-animal variability at that time point. The dose level of abatacept did not seem to be limiting, given that mean serum concentrations of acazicolcept were 46% and 71% lower than those of abatacept at Day 18 and Day 29 (2 hr post-dose), 85% lower at Day 29 pre-dose, and 80% lower at Day 34 (120 hr post

dose 5) (data not shown). The lack of robust activity with abatacept may be due to the delayed dosing (Day 18) in the current study since greater activity has been observed with 5 mg/kg mouse CTLA-4-Ig administered in a prophylactic setting (Day 0) (37).

Mice treated with acazicolcept or abatacept had significantly lower concentrations of anti-mouse collagen IgG antibodies on Day 34 compared with DPBS-treated mice (p=0.0015 vs. acazicolcept; p=0.0162 vs. abatacept) or Fc control-treated mice (p=0.0056 vs. acazicolcept, p=0.049 vs. abatacept) (Figure 2C). There was no significant difference in anti-collagen IgG antibody concentrations between the acazicolcept and abatacept treatment groups (p>0.99).

Histological analysis (Figure 2D-E and Supplementary Figure 1C) demonstrated that paws from acazicolcept-treated mice had significantly less inflammation, pannus formation, cartilage damage, and bone resorption compared with paws from the DPBS or Fc control groups (p<0.0001 for each endpoint and as a composite score), whereas abatacept treatment only modestly reduced cartilage damage (p=0.0446) and bone resorption (p=0.031) compared to DPBS.

Flow cytometry analysis of the popliteal lymph node (LN) cells collected at study termination on Day 34 was performed to investigate treatment impact on various lymphocyte subsets in the paw draining LN (Figure 2F). Compared with the DPBS or Fc control groups, both acazicolcept and abatacept significantly reduced

percentages of CXCR5+PD-1+CD4+ follicular helper T (T_{FH}) cells and CD19+GL-7+ GC B cells. Acazicolcept significantly reduced the percentage of CD4+ and CD8+ T cells (data not shown) producing intracellular IL-17A, and the percentage of CD4+ (but not CD8+) T cells producing IFNγ, compared with the DPBS and Fc control groups, and also reduced the percentage of IL-17A+ and IFNγ+ CD4+ T cells compared to the abatacept-treated groups (p=0.073 and p=0.0189, respectively) (Figure 2F). Finally, serum cytokines were measured at study termination (Figure 2G-H). Compared to mice treated with Fc control, acazicolcept-treated mice had significantly reduced levels of IL-6, IL-13, IL-17A, and TNFα, while abatacept-treated mice had significantly reduced concentrations of IL-6 and IL-13, as summarized in the heat map in Figure 2H. Levels of circulatingIL-6, IL-13, IL-17A, and TNFα were all significantly reduced in the acazicolcept group compared with the abatacept-treated mice (p<0.0001, p=0.0007, p=0.035, and p=0.005, respectively).

Acazicolcept inhibits cytokine secretion from stimulated patient or healthy donor PBMCs

Cytokines produced by activated T cells and myeloid cells have been associated with pathology in both RA and PsA, and therapeutics specifically neutralizing such molecules, including TNFα, IL-1, IL-6, IL-12/23, and IL-17, have shown promise in the treatment of RA and/or PsA (38).

PBMC from 13 RA or 15 PsA patients with confirmed clinical diagnoses or 10 healthy donors (Supplementary Table 1) were evaluated for their cytokine response to CD28- and ICOS-mediated costimulation in the presence or absence of acazicolcept or comparators. PBMC were stimulated with aAPCs expressing cell-surface OKT3 scFv (anti-CD3), and human CD80, CD86, and ICOSL. PBMC, aAPCs, and test articles (100 nM) (Figure 3A) were co-cultured for 48 hours. Supernatants were collected, and levels of IFNγ, IL-2, and IL-6 were each determined individually by ELISA, while IL-13, IL-17A, IL-17F, IL-21, GM-CSF, TNFα, IL-12p70, and IL-1β were measured by multiplex analysis. RNA was also isolated from harvested stimulated PBMC for RNAseq analysis. While other immunomodulatory proteins such as IL-10 and FoxP3 were not included in the multiplex analysis, their RNA expression was evaluated. There was a significant (p=0.0221) decrease in *IL10* gene expression for acazicolcept treatment vs. Fc control in the PsA, but not RA (p=0.0764), PBMC cultures, and we observed a significant increase in *FOXP3* gene expression in both the RA (p<0.0001) and PsA (p=0.0004) PBMC cultures containing acazicolcept (vs. Fc control) (data not shown).

Compared to treatment with Fc control, abatacept, or prezalumab, acazicolcept demonstrated superior cytokine inhibition for all cytokines tested (except for IL-1β, not shown), including select arthritis-associated inflammatory cytokines IFNγ, IL-17A, and TNFα (Figure 3B), for nearly all donors evaluated. Prezalumab modestly inhibited only IL-13 and IL-17A production in all PBMC types, while the combination of abatacept and prezalumab yielded somewhat greater inhibition

of IL-2, IL-21, IL-12p70, IL-13, IL-17A, IL-17F, GM-CSF, and IFNγ compared to Fc control or either inhibitor alone (Figure 3C).

Strikingly, acazicolcept demonstrated significant and enhanced cytokine suppression even compared to the combination of abatacept and prezalumab for all cytokines tested except IL-13 and IL-17A, for which inhibition by acazicolcept and the combination treatment was similar. These results suggest that co-inhibition of both CD28 and ICOS pathways yields greater suppression of these cytokines than blockade of either pathway alone. Furthermore, acazicolcept modulates a broader spectrum of inflammatory cytokines than the combination of biologics individually targeting the CD28 and ICOS pathways.

Acazicolcept inhibits multiple inflammatory genes in PsA and RA

To assess more broadly the impact of acazicolcept treatment in the human PBMC/aAPC co-cultures, RNA was isolated from cells harvested at the end of the culture period and RNASeq analysis was conducted. Consistent with its effects on secreted cytokines (Figure 3), acazicolcept significantly suppressed expression of multiple genes, including those encoding inflammatory cytokines such as *IL17A*, *IL17F*, *TNF*, *IFNG*, and *IL6*, in PBMC from RA (Supplementary Figure 2A) and PsA (Supplementary Figure 2B) patients compared to the other treatments evaluated. While transcript levels for all these pathogenic cytokines were reduced by treatment with abatacept and the combination of abatacept+prezalumab, the inhibition observed with acazicolcept was even more dramatic. In fact, a statistically significant reduction in transcripts from acazicolcept-treated cultures

was measured for all five cytokines relative to treatment with abatacept+prezalumab (per estimation plots shown in Supplementary Figure 2).

In line with its proposed mechanism of action, acazicolcept also prevented an increase in the expression of genes encoding ICOS and PD-1, which are both typically upregulated upon T cell activation, while preventing downregulation of CD28 gene expression in PBMC from both RA (Supplementary Figure 3A) and PsA (Supplementary Figure 3B) patients.

Next, we explored transcriptome-wide changes across donor types in the absence of aAPC stimulation. Principal component analysis (PCA) plots revealed that unstimulated PBMC healthy donor (HD) samples had a distinct transcriptional profile compared to PBMC from RA or PsA patients (Supplementary Figure 4A). Using differential expression analysis, we compared HD vs. RA (Supplementary Figure 4B) or HD vs. PsA (Supplementary Figure 4C) to identify genes that were significantly altered between donor types. PBMC from PsA patients showed a transcriptional signature distinct from the other PBMC types in the absence of aAPC stimulation. Two of the RA donors clustered with PsA donors on the PCA plot (Supplementary Figure 4A); this could not be explained by any clear pattern in their disease scores or treatments at time of PBMC donation (Supplementary Table 1). Prior to treatment, PsA (but not RA) PBMC expressed more genes associated with T cell activation (e.g., IL2, GZMB, IFNG) as compared to HD

PBMC, suggesting they might be more responsive to a T cell inhibitor (Supplementary Figure 4A).

To identify a transcriptional signature consistent with acazicolcept treatment, we performed differential gene expression analysis between Fc control- and acazicolcept-treated aAPC/PBMC co-cultures from each of the three donor types (HD, RA, and PsA). A Venn diagram was used to compare all the genes that were significantly downregulated following acazicolcept treatment across each donor type, and revealed that acazicolcept inhibited the expression of multiple genes related to immune responses and disease pathogenesis (Figure 4A). Sixty-three genes (including *CD40LG*, *ICOS*, *IFNG*, *IL17A*, *IL17F*, *IL2*, *ICOS*, *IL21*, and *PDCD1*) were significantly decreased with acazicolcept treatment across all donor types (Figure 4A), suggesting a core acazicolcept gene signature. Differential expression analysis was then used to identify shared genes that were significantly downregulated by both acazicolcept and various treatments compared to Fc controls in either RA (Figure 4B) or PsA (Figure 4C) patient PBMCs. Notably, all three treatment types reduced the expression of *IL2*, *IL21*, and *NFKBID* in both RA (Figure 4B) and PsA (Figure 4C) donor PBMC cultures. Compared to Fc control, treatment with either acazicolcept or abatacept+prezalumab reduced the expression of multiple genes previously linked to arthritic disease, including *IL17A*, *CCL17*, *CCL20*, *IL4* and *PDCD1*, in both donor types (Figure 4B-C).

To understand how acazicolcept differs from abatacept+prezalumab, we used PCA plots to visualize global transcriptional differences between treatments for each of the PBMC donor types (Figure 5A). While acazicolcept and the combination treatment induced a similar transcriptional pattern in HD PBMC, acazicolcept impacted a slightly broader set of genes than abatacept+prezalumab in the RA PBMC but mediated a clearly disparate set of transcriptional changes in the PsA PBMC (Figure 5A). Differential expression analysis revealed that acazicolcept more potently suppressed transcription of genes related to inflammation and T cell activation, such as *CCL3L3*, *IL2, IL22, IL17F*, *IL17A*, *IL1R1, SOCS3*, *LIF, OSM, IFNG, CTLA4, ICOS,* and *IL21*, compared to abatacept+prezalumab in PsA patients (Figure 5B-D). The top 25 downregulated genes are visualized in the heatmap from Figure 5E. Many of the genes that emerged as more highly expressed in the acazicolcept-treated (vs. abatacept+prezalumab-treated) PBMC were myeloid-related (e.g., *LYZ*, *ITGAX*, *HLA-DRB1*) and this signature is likely more dominant when T cell activation is suppressed by acazicolcept (Figure 5B, Supplementary Figure 4D). Notably, prezalumab had relatively little impact on the transcriptional profile in the co-cultures, and the profile observed with abatacept+prezalumab vs. acazicolcept was similar to that of abatacept alone vs. acazicolcept (Figure 5C-D). Cell type skewing is unlikely to be driving the transcriptional changes in our dataset, as many immune-cell specific lineage genes and MKI67 (Ki-67), which is important for cell proliferation, were relatively equivalent across the different treatment conditions (Supplemental Figure 4D-E). Finally, application of the IPA program

to gain more insight into canonical pathways affected by treatment with acazicolcept, given the pattern of differentially expressed genes, predicted that multiple pathways linked to IL-17 signaling would be decreased following treatment with acazicolcept compared to treatment with abatacept+prezalumab (Figure 5F, Supplementary Figure 4F).

Taken together, these analyses suggest that acazicolcept can inhibit the expression of pathogenic genes and/or pathways implicated across multiple immune response and inflammatory disease settings, and that acazicolcept inhibits the CD28 and ICOS costimulation pathways more effectively than the combination of the single pathway inhibitors abatacept and prezalumab.

DISCUSSION

The most striking result of our studies is the clear differentiation between acazicolcept co-blockade of the CD28 and ICOS pathways and antagonism of the same two pathways with a combination of abatacept and prezalumab. There are likely several reasons for this differentiation. Acazicolcept was designed to directly bind with high affinity to CD28 and ICOS on T cells and inhibit their interactions with CD80/CD86 and ICOSL, respectively, on APC. Conversely, abatacept and prezalumab bind respectively to CD80/CD86 or ICOSL on APC. Moreover, the affinity of acazicolcept for its targets is higher than that of abatacept or prezalumab for their targets, enabling better blockade of both the CD28 and ICOS pathways (Figure 1C-E). The specific 3-dimensional binding

epitopes of acazicolcept on CD28 and ICOS may also position the drug to disrupt interactions with their cognate receptors more efficiently than abatacept or prezalumab. The smaller size of acazicolcept (~80 kD) compared to two 150-kD mAbs may be another factor impacting its improved potency, as it should be less sterically hindered from accessing and blocking CD28 and ICOS within the immune synapse.

Naïve T cells generally express CD28 but little to no ICOS, and following antigen encounter most activated T cells become CD28+ ICOS+. However, a subset of activated T cells downregulates CD28 and become $CD28^{low}$ ICOS+ or CD28- ICOS+; such cells account for up to half of the total circulating T cell population in the elderly. CD28- ICOS+ cells are resistant to CTLA-4-Fc therapy and appear to play important roles in inflammatory and autoimmune diseases (39-42). We found that addition of acazicolcept to PBMC/aAPC cultures prevented an increase in the expression of genes encoding ICOS and PD-1, both typically upregulated upon T cell activation, while preventing downregulation of CD28 gene expression in PBMC from both RA and PsA patients (Supplementary Figure 2). Similar effects of acazicolcept treatment on the expression of ICOS, PD-1, and CD28 were previously observed for human T cells isolated from a humanized mouse model of acute GVHD (31). Thus, one mechanism of action of acazicolcept may be to inhibit the emergence of activated ICOS+CD28+ pathogenic T cells that escape CD28 single pathway blockade.

In this regard, our data from the CIA model and the human PBMC translational studies clearly demonstrate that co-inhibition of CD28 and ICOS by acazicolcept is more effective than inhibitors of either pathway alone or combined. The impact of CD28 and ICOS dual inhibition by acazicolcept on Th17 cells and their secreted products (IL-17A, IL-17F) and transcriptional pathways was particularly notable and may further emphasize the role of ICOS in Th17 biology (17, 43). Indeed, IL-17A was one of the few genes impacted by prezalumab when it was added to abatacept in the PBMC/aAPC co-cultures (Figure 5D). From the significant reductions in Th17 cells in the draining LN and in serum IL-17A in the mouse CIA model (Figure 2H-J), to the suppression of secreted IL-17A and IL-17F and significantly decreased transcription of Th17-related genes in the human PBMC cultures (Figures 3-5; Supplementary Figures 1-2), our data show that blockade of CD28 and ICOS by acazicolcept dramatically impacts the Th17 pathway. RNASeq and pathway analyses revealed the additional impact of acazicolcept on the Th1, Th2, and HMGB1 signaling pathways (Figure 5F), each of which have previously been identified as potential targets for the treatment of arthritis (44), and reductions in Th1 (TNFα) and Th2 (IL-13) cytokines were also observed in the CIA model (Figure 2). These findings suggest that acazicolcept might be an effective treatment for IL-17–driven arthritis, such as PsA or other spondyloarthropathies.

Additional genes associated with PsA and RA pathogenesis, including co-stimulatory molecules and inflammatory Th2-associated effectors, were more

significantly downregulated by acazicolcept than by comparators (Figures 4-5). Taken together, the effects of dual CD28/ICOS blockade by acazicolcept seem particularly relevant to PsA, where inhibition of the CD28 pathway with abatacept has not been a preferred treatment due to its relative lack of efficacy in multiple domains, such as axial disease (45).

The limitations of these studies include the inherent caveats associated with any animal model for human disease. The mouse CIA model does not fully reproduce the human clinical pathology and induces acute rather than chronic arthritis; nevertheless, it is generally considered a standard model for studies of arthritis (36, 37). In addition, treatment of patient PBMC ex vivo may not fully reflect the effects of treatment on affected tissues in vivo, and PBMC from different donors will likely have different immune cell compositions which could impact the RNAseq results. Furthermore, our cytokine multiplex analysis was mostly limited to Type 1/2/17 cytokines and did not include anti-inflammatory/ immunoregulatory molecules like IL-10, TGFβ, or FoxP3, though we did capture those in the gene expression analysis. Further, the RA patient PBMC donors used for this study were not as diverse as the PsA PBMC donors. The RA patients were heavily pre-treated, their PBMC generally had lower overall viability in the co-cultures regardless of treatment, and they were not as strongly activated by the aAPC as were the PsA PBMC (Supplementary Table 1 and Supplementary Figure 3). These factors limited our ability to make definitive distinctions between the RA and PsA donor sets. However, despite these limitations, the correlation

between findings in the CIA model and the human PBMC assays support clinical translatability of our results.

Our findings suggest that acazicolcept, by inhibiting both the CD28 and ICOS pathways, may be a promising therapeutic approach to inflammatory arthritis conditions such as PsA and RA, potentially yielding improved and perhaps more durable efficacy outcomes. In adult healthy volunteers, acazicolcept has been well tolerated with dose-dependent pharmacokinetics and pharmacodynamic effects on assessments such as SEB-mediated T cell activation and responses to KLH immunization, consistent with its designed mechanism of action (46). Clinical studies with acazicolcept in inflammatory arthritis, particularly PsA, may therefore be of particular interest.

Acknowledgements: We thank our past and present Alpine Immune Sciences colleagues, and particularly Dan Ardourel, Dr. Heidi LeBlanc, Dr. Jing Yang, Dr. Jan L. Hillson, Elizabeth Repash, and Erika Rickel, for their contributions to this work. We also thank Hooke Laboratories for their excellent conduct of the CIA model, and Mary Derry and Julie Crider for their assistance with preparation of the manuscript.

REFERENCES

1. Choy E. T cells in psoriatic arthritis. Curr Rheumatol Rep 2007;9:437-41.

2. Cope AP. T cells in rheumatoid arthritis. Arthritis Res Ther 2008;10 Suppl 1:S1.

3. Yao S, Zhu Y, Chen L. Advances in targeting cell surface signalling molecules for immune modulation. Nat Rev Drug Discov 2013;12:130-46.

4. Rudd CE, Schneider H. Unifying concepts in CD28, ICOS and CTLA4 co-receptor signalling. Nat Rev Immunol 2003;3:544-56.

5. Liu M, Yu Y, Hu S. A review on applications of abatacept in systemic rheumatic diseases. Int Immunopharmacol 2021;96:107612.

6. Watkins B, Qayed M, McCracken C, et al. Phase II trial of costimulation blockade with abatacept for prevention of acute GVHD. J Clin Oncol 2021;39:1865-77.

7. de Jong YP, Rietdijk ST, Faubion WA, et al. Blocking inducible co-stimulator in the absence of CD28 impairs Th1 and CD25+ regulatory T cells in murine colitis. Int Immunol 2004;16:205-13.

8. Pontarini E, Verstappen GM, Grigoriadou S, et al. Blocking T cell co-stimulation in primary Sjögren's syndrome: rationale, clinical efficacy and modulation of peripheral and salivary gland biomarkers. Clin Exp Rheumatol 2020;38 Suppl 126:222-7.

9. Gao X, Gigoux M, Yang J, et al. Anti-chlamydial Th17 responses are controlled by the inducible costimulator partially through phosphoinositide 3-kinase signaling. PLoS One 2012;7:e52657.

10. Wekerle T, Grinyó JM. Belatacept: from rational design to clinical application. Transpl Int 2012;25:139-50.

11. Kremer JM, Westhovens R, Leon M, et al. Treatment of rheumatoid arthritis by selective inhibition of T-cell activation with fusion protein CTLA4Ig. N Engl J Med 2003;349:1907-15.

12. Mease PJ, Gottlieb AB, van der Heijde D, et al. Efficacy and safety of abatacept, a T-cell modulator, in a randomised, double-blind, placebo-controlled, phase III study in psoriatic arthritis. Ann Rheum Dis 2017;76:1550-8.

13. Ruperto N, Lovell DJ, Quartier P, et al. Abatacept in children with juvenile idiopathic arthritis: a randomised, double-blind, placebo-controlled withdrawal trial. Lancet 2008;372:383-91.

14. Poirier N, Blancho G, Vanhove B. Alternatives to calcineurin inhibition in renal transplantation: belatacept, the first co-stimulation blocker. Immunotherapy 2010;2:625-36.

15. Masson P, Henderson L, Chapman JR, et al. Belatacept for kidney transplant recipients. Cochrane Database Syst Rev 2014;2014:Cd010699.

16. Singh JA, Hossain A, Mudano AS, et al. Biologics or tofacitinib for people with rheumatoid arthritis naive to methotrexate: a systematic review and network meta-analysis. Cochrane Database Syst Rev 2017;5:Cd012657.

17. Wikenheiser DJ, Stumhofer JS. ICOS Co-stimulation: friend or foe? Front Immunol 2016;7:304.

18. Weber JP, Fuhrmann F, Feist RK, et al. ICOS maintains the T follicular helper cell phenotype by down-regulating Krüppel-like factor 2. J Exp Med 2015;212:217-33.

19. Esposito P, Grosjean F, Rampino T, et al. Costimulatory pathways in kidney transplantation: pathogenetic role, clinical significance and new therapeutic opportunities. Int Rev Immunol 2014;33:212-33.

20. Panneton V, Chang J, Witalis M, et al. Inducible T-cell co-stimulator: Signaling mechanisms in T follicular helper cells and beyond. Immunol Rev 2019;291:91-103.

21. Fonseca VR, Romão VC, Agua-Doce A, et al. The ratio of blood T follicular regulatory cells to T follicular helper cells marks ectopic lymphoid structure formation while activated follicular helper T cells indicate disease activity in primary Sjögren's syndrome. Arthritis Rheumatol 2018;70:774-84.

22. Sato T, Kanai T, Watanabe M, et al. Hyperexpression of inducible costimulator and its contribution on lamina propria T cells in inflammatory bowel disease. Gastroenterology 2004;126:829-39.

23. Cheng LE, Amoura Z, Cheah B, et al. Brief report: a randomized, double-blind, parallel-group, placebo-controlled, multiple-dose study to evaluate AMG 557 in patients With systemic lupus erythematosus and active lupus arthritis. Arthritis Rheumatol 2018;70:1071-6.

24. Choi JY, Ho JH, Pasoto SG, et al. Circulating follicular helper-like T cells in systemic lupus erythematosus: association with disease activity. Arthritis Rheumatol 2015;67:988-99.

25. Wang J, Shan Y, Jiang Z, et al. High frequencies of activated B cells and T follicular helper cells are correlated with disease activity in patients with new-onset rheumatoid arthritis. Clin Exp Immunol 2013;174:212-20.

26. Romme Christensen J, Börnsen L, Ratzer R, et al. Systemic inflammation in progressive multiple sclerosis involves follicular T-helper, Th17- and activated B-cells and correlates with progression. PLoS One 2013;8:e57820.

27. Mariette X, Bombardieri M, Alevizos I, et al. A phase 2a study of MEDI5872 (AMG557), a fully human anti-ICOS ligand monoclonal antibody in patients with primary Sjögren's syndrome (Abstract). Arthritis Rheumatol 2019;71, Suppl.10.

28. Nanji SA, Hancock WW, Anderson CC, et al. Multiple combination therapies involving blockade of ICOS/B7RP-1 costimulation facilitate long-term islet allograft survival. Am J Transplant 2004;4:526-36.

29. Wong SC, Tan AH, Lam KP. Functional hierarchy and relative contribution of the CD28/B7 and ICOS/B7-H2 costimulatory pathways to T cell-mediated delayed-type hypersensitivity. Cell Immunol 2009;256:64-71.

30. Li J, Semple K, Suh WK, et al. Roles of CD28, CTLA4, and inducible costimulator in acute graft-versus-host disease in mice. Biol Blood Marrow Transplant 2011;17:962-9.

31. Adom D, Dillon SR, Yang J, et al. ICOSL(+) plasmacytoid dendritic cells as inducer of graft-versus-host disease, responsive to a dual ICOS/CD28 antagonist. Sci Transl Med 2020;12.

32. Orvain C, Cauvet A, Prudent A, et al. Acazicolcept (ALPN-101), a dual ICOS/CD28 antagonist, demonstrates efficacy in systemic sclerosis preclinical mouse models. Arthritis Res Ther 2022;24:13.

33. Levin SD, Evans LS, Bort S, et al. Novel immunomodulatory proteins generated via directed evolution of variant IgSF domains. Front Immunol 2019;10:3086.

34. Bernett MJ, Chu SY, Leung I, et al. Immune suppression in cynomolgus monkeys by XPro9523: an improved CTLA4-Ig fusion with enhanced binding to CD80, CD86 and neonatal Fc receptor FcRn. MAbs 2013;5:384-96.

35. Patakas A, Ji RR, Weir W, et al. Abatacept inhibition of T cell priming in mice by induction of a unique transcriptional profile that reduces their ability to activate antigen-presenting cells. Arthritis Rheumatol 2016;68:627-38.

36. Choudhary N, Bhatt LK, Prabhavalkar KS. Experimental animal models for rheumatoid arthritis. Immunopharmacol Immunotoxicol 2018;40:193-200.

37. Webb LM, Walmsley MJ, Feldmann M. Prevention and amelioration of collagen-induced arthritis by blockade of the CD28 co-stimulatory pathway: requirement for both B7-1 and B7-2. Eur J Immunol 1996;26:2320-8.

38. Luchetti MM, Benfaremo D, Gabrielli A. Biologics in inflammatory and immunomediated arthritis. Curr Pharm Biotechnol 2017;18:989-1007.

39. Betjes MG. Clinical consequences of circulating CD28-negative T cells for solid organ transplantation. Transpl Int 2016;29:274-84.

40. Schmidt D, Goronzy JJ, Weyand CM. CD4+ CD7- CD28- T cells are expanded in rheumatoid arthritis and are characterized by autoreactivity. J Clin Invest 1996;97:2027-37.

41. Garin L, Rigal D, Souillet G, et al. Strong increase in the percentage of the CD8bright+ CD28- T-cells and delayed engraftment associated with cyclosporine-induced autologous GVHD. Eur J Haematol 1996;56:119-23.

42. de Graav GN, Hesselink DA, Dieterich M, et al. Down-regulation of surface CD28 under belatacept treatment: an escape mechanism for antigen-reactive T-cells. PLoS One 2016;11:e0148604.

43. Paulos CM, Carpenito C, Plesa G, et al. The inducible costimulator (ICOS) is critical for the development of human T(H)17 cells. Sci Transl Med 2010;2:55ra78.

44. Kaur I, Behl T, Bungau S, et al. Exploring the therapeutic promise of targeting HMGB1 in rheumatoid arthritis. Life Sci 2020;258:118164.

45. Singh JA, Guyatt G, Ogdie A, et al. Special Article: 2018 American College of Rheumatology/National Psoriasis Foundation Guideline for the Treatment of Psoriatic Arthritis. Arthritis Rheumatol 2019;71:5-32.

46. Yang J, Lickliter JD, Hillson JL, et al. First-in-human study of the safety, tolerability, pharmacokinetics, and pharmacodynamics of ALPN-101, a dual CD28/ICOS antagonist, in healthy adult subjects. Clin Transl Sci 2021;14:1314-26.

FIGURE LEGENDS

Figure 1. Acazicolcept (ALPN-101) is a dual CD28/ICOS antagonist that suppresses two key T cell costimulation pathways

A. Schematic of acazicolcept, comprising a variant ICOSL domain generated by directed evolution. **B.** Mechanism of action of acazicolcept and comparators. CD28 and ICOS costimulation results in T cell activation. These pathways are separately inhibited by CTLA-4-Ig (abatacept and belatacept, which bind CD80 and CD86 and prevent their interaction with CD28 or CTLA-4) and the anti-ICOSL mAb prezalumab. Acazicolcept binds both CD28 and ICOS, though not necessarily simultaneously, and inhibits both pathways. **C.** Acazicolcept binds CD28 and ICOS. Acazicolcept was incubated with CHO cells expressing human CD28 (*upper*) or ICOS (*lower*). Bound protein was detected with anti-human IgG-PE and measured by flow cytometry. Median fluorescence intensity is plotted versus acazicolcept concentration (pM). **D.** Acazicolcept or comparators were incubated with fixed amounts of CD80, CD86 or ICOSL labeled with AF647. Test articles were incubated with CHO cells expressing human CD28 (*upper*) or $ICOS_{ECD}/CD28_{ICD}$ (*lower*) and bound CD80-, CD86-, or ICOSL-AF647 was measured by flow cytometry to determine IC_{50} levels. **E.** Effect of acazicolcept and comparators on CD28 (*upper*) and ICOS co-stimulation (*lower*). Data are representative of ≥10 (**B**) or ≥2 (**C-E**) experiments.

Figure 2. Acazicolcept is more effective than abatacept in a mouse collagen-induced arthritis (CIA) model

Mice were treated every 3 days for 5 total doses with vehicle (DPBS), 0.5 mg acazicolcept or abatacept, or 0.312 mg (molar-matched) Fc control, starting on Day 18. **A.** Percent initial body weight over time. **B.** CIA paw scores over time (see Methods for scoring details). **C.** Anti-mouse collagen IgG serum concentrations (μg/mL) at termination (Day 34) (*p<0.05, **p<0.01). **D, E.** Paws collected at termination were formalin fixed and decalcified for histological analysis. **D.** Representative images of paws stained with toluidine blue (10× magnification, bar=500 μm). C, carpal bone(s); M, metacarpal bone(s); R, radius; SI, synovial inflammation; U, ulna. **E.** Stained paw sections were analyzed and scored. Sum of paw histology scores for individual parameters in Supplementary Figure 1C is shown for each treatment group (**** p<0.0001). **F.** Percentages (mean ± SD) of indicated lymphocyte subsets in popliteal lymph nodes on Day 34, determined by flow cytometry (*p<0.05, **p<0.01, ****p<0.0001). **G.** Serum cytokines for DPBS-treated mice on Day 34. **H.** Effects of Fc control, abatacept, and acazicolcept on serum cytokines, relative to DPBS-treated mice. Representative results from 3 CIA studies are shown.

Figure 3. Acazicolcept demonstrates superior inhibition over single pathway inhibitors of cytokine secretion from stimulated RA or PsA patient or healthy donor PBMC

Patient or healthy donor PBMC were stimulated with fixed aAPC (K562 cells expressing OKT3 scFv, CD80, CD86, and ICOSL) for 48 hours in the presence of acazicolcept (100 nM) or comparators, and cytokine secretion in the culture

supernatants was measured by ELISA or multiplex analysis, as detailed in Materials and Methods. **A**. Schematic of PBMC/aAPC co-cultures and test articles with corresponding targets that were evaluated for cytokine secretion. **B.** Concentrations of IFNγ, IL-17A, and TNFα are plotted for each PBMC donor; horizontal black bars represent the mean values for each group. **C.** Heat map showing relative inhibition of the full panel of cytokines evaluated.

Figure 4. Gene expression in human PBMC/aAPC co-cultures is differentially impacted by acazicolcept, abatacept, and abatacept combined with prezalumab.

RNA was isolated from PBMC/aAPC co-cultures as described in Fig. 3, and subsequently used for RNASeq analysis. **A.** Venn diagram comparing all genes significantly downregulated by acazicolcept compared to Fc control in each of the 3 PBMC types evaluated (HD, RA, and PsA). A list of the 63 genes impacted in all 3 PBMC donor types is provided to the right of the Venn diagram. **B-C.** Venn diagrams comparing genes from **(B)** RA or **(C)** PsA PBMC cultures that were decreased with treatment by Fc control compared to acazicolcept, abatacept, or abatacept+prezalumab. The **(B)** 9 genes in RA or **(C)** 28 genes in PsA that were significantly decreased by all 3 treatment types compared to Fc controls are listed on the right. The **(B)** 30 genes in RA and **(C)** 35 genes in PsA that were only decreased with acazicolcept and abatacept+prezalumab are listed on the left. For each comparison, differentially expressed genes with a BH-adjusted p value <0.05 and absolute value fold change >1.5 were considered significant.

Figure 5. Acazicolcept suppresses the expression of genes associated with T cell activation more potently than combination treatment with abatacept and prezalumab.

RNA was isolated from cells harvested from the PBMC/aAPC co-cultures described in Figure 3 and subjected to RNASeq analysis, as described in Materials and Methods. **A.** Vst-transformed raw gene counts were plotted using PCA analysis for HD, RA, and PsA patient PBMCs/aAPC co-cultures treated with either acazicolcept or abatacept+prezalumab. **B-D.** Differentially expressed genes in PsA PBMC cultures for abatacept+prezalumab vs. acazicolcept (**B**), abatacept vs. acazicolcept (**C**), or abatacept vs. abatacept+prezalumab (**D**). Genes were plotted using a volcano plot and differentially expressed genes with a BH-adjusted *p* value <0.05 (horizontal dashed line) and absolute value fold change >1.5 (vertical dashed line) were considered significant (yellow dots). **E.** Heatmap with z-score of transcripts per million (TPM) for the top 25 genes that were significantly downregulated with acazicolcept compared to abatacept+prezalumab treatment. **F.** Differentially expressed genes from **B** were input into Ingenuity Pathway Analysis (IPA) from Qiagen to identify canonical pathways that were downregulated with acazicolcept relative to abatacept+prezalumab. Pathways with IPA z-score < -2 and BH adjusted *p* value < 0.1 were considered significant.

SUPPLEMENTARY METHODS

Acazicolcept and comparators

Acazicolcept is a dimer of a ICOSL vIgD domain fused to an effectorless IgG1 Fc. The generation of acazicolcept was previously described (31, 33). Acazicolcept was produced at KBI Biopharma (Durham, NC). Nulojix® (belatacept) and Orencia® (abatacept) were purchased from Catalent (Somerset, NJ), and anti-ICOSL mAb (prezalumab) was purchased from Creative Biolabs (Shirley, NY). A WT ICOSL-Fc fusion protein with the same structure as acazicolcept, and an Fc control protein comprising the same Fc sequence used in acazicolcept, were produced at Alpine Immune Sciences.

Binding of acazicolcept to CD28 and ICOS and inhibition of ligand binding

To measure binding to CD28 and ICOS, acazicolcept or comparators were titrated and incubated with Chinese hamster ovary (CHO) cells transfected with human CD28 or ICOS, detected with anti-human IgG-PE, and measured by flow cytometry. To demonstrate blockade of CD28 and ICOS to their respective ligands, acazicolcept or comparators were titrated and incubated with fixed amounts of CD80, CD86, or ICOSL labeled with AlexaFluor (AF)-647 (ThermoFisher Scientific) and added to CHO cells expressing human CD28 or ICOS. After incubation for 60 minutes, samples were washed and assessed by flow cytometry. EC_{50} and IC_{50} values were determined using GraphPad Prism.

Costimulation assay for functional characterization of acazicolcept

Artificial antigen presenting cells (aAPC) were generated by transducing K562 cells (ATCC CCL-243) with lentivirus to express cell surface anti-human CD3

single chain variable fragment (OKT3 scFv) and full-length human CD80, and/or CD86, and/or ICOSL (K562/OKT3/CD80/CD86/ICOSL). Cell surface transgene expression was confirmed by flow cytometry. Jurkat/IL-2 effector cells expressing endogenous CD28 and a transduced luciferase gene driven by an IL-2 promoter (Promega) were used to measure CD28-mediated costimulation. An ICOS transmembrane and extracellular domain (ECD)/CD28 intracellular domain (ICD) chimeric receptor ($ICOS_{ECD}/CD28_{ICD)}$ was transduced into Jurkat/IL-2 cells to measure ICOS-mediated costimulation. To measure CD86–CD28 or ICOSL–ICOS blockade, acazicolcept or comparators were titrated and added to wells containing 2.5×10^4 aAPCs in Jurkat Assay Buffer (RPMI 1640 + 5% FBS) for 15–30 minutes at RT with shaking. Jurkat/IL-2 or ICOS-CD28 effector cells were added at 1.25×10^5 cells per well. After 5 hours incubation at 37°C with 5% CO_2 and cell lysis, plates were developed with luciferase substrate solution (BioGlo luciferase reagent; Promega). Relative light units (RLU) were determined by measuring luminescence on a Cytation 3 imaging reader (BioTek Instruments).

Mouse Collagen-Induced Arthritis Model

Animals and Treatments

All experiments in mice were performed under a protocol approved by Hooke Laboratories' Institutional Animal Care and Use Committee (IACUC; Protocol #1909 Arthritis) and carried out according to the Guide for the Care and Use of Laboratory Animals. Mice were housed at 24 ± 2°C on a 12-hour light/12-hour dark cycle with free access to food and water at all times. Male DBA/1 mice

(Taconic Biosciences, Germantown, NY) (N=60) were immunized via subcutaneous (SC) tail injection on Day 0 with bovine collagen in Complete Freund's adjuvant (CFA) (EK-0220 emulsion prepared by Hooke Laboratories; Lawrence, MA), and then boosted with bovine collagen in incomplete Freund's adjuvant (IFA) (EK-0221 emulsion; Hooke Laboratories) on Day 18. Mice were randomized on Day 18, prior to the collagen boost, to create groups with similar average body weight at the time of treatment start (average body weight was within 0.9 g between the groups); none of the mice exhibited clinical signs of CIA at that time. Group size (N=15) was based on Hooke Laboratory's experience with this model, enabling consistent observation of efficacy with a moderately potent positive control (anti-TNF mAb). Two mice were excluded from the study: one from the vehicle group was excluded due to an injured front paw, and one mouse in the abatacept group died due to complications of the collagen booster immunization. Mice were injected intraperitoneally (IP) every 3 days for a total of 5 doses with vehicle (Dulbecco's phosphate buffered saline/DPBS), Fc control, abatacept, or 0.5 mg (~20 mg/kg) acazicolcept, or molar-matched dose levels of Fc control (0.312 mg) or abatacept (0.5 mg) in a semi-therapeutic regimen, starting just before administration of the collagen boost on Day 18. Treatments were always administered in the same order, cage location was not changed during the study, and mice treated with different treatments were not co-housed. Location of cages was randomized before scoring, and scoring was performed blind in a different order by different scientists during the study. The project manager and staff administering treatment were aware of the group

allocation. Clinical scoring was performed by scientists blind to treatment conditions and previous clinical scores. Serum was collected at various time points for assessment of drug exposure, anti-drug antibodies (ADA), anti-collagen antibodies, and cytokines. Arthritis scores and body weight were recorded until the end of the study (Day 34 after first collagen immunization). Each mouse was sacrificed after the final clinical scoring on Day 34 for endpoint assessments.

Body weights and disease activity scoring

Body weights were collected for each mouse every 2–3 days throughout the study. Mice were scored for disease activity every other day starting on Day 14, on a scale of 0–16 (0–4 for each paw, adding the scores for all 4 paws), according to the following system: 0, normal paw; 1, one toe inflamed and swollen; 2, more than one toe, but not entire paw, inflamed and swollen OR mild swelling of entire paw; 3, entire paw inflamed and swollen; 4, very inflamed and swollen paw or ankylosed paw. CIA paw scoring was performed in a blinded fashion.

Anti-collagen antibodies

Reactivity of DBA/1 mice to mouse collagen type II was determined using commercial ELISA kits (Chondrex; Redmond, WA) to measure serum levels of total mouse IgG antibodies (cat. #2036T) and mouse IgG2a-isotype antibodies (cat. #20362T), per the manufacturer's instructions.

Serum cytokine analysis

Serum samples were thawed, vortexed, and centrifuged at 14,000 rpm, 4°C for 5 minutes prior to conducting assays. Cytokines were measured using MILLIPLEX® MAP Mouse High Sensitivity T Cell Magnetic Bead Panel multiplex assay, cat# MHSTCMAG-70K-10, from EMD Millipore. Samples were diluted as needed (1:2 to 1:6) in the manufacturer's assay diluent and assayed according to the manufacturer's protocol. Average serum cytokine levels were first determined for DPBS-treated mice, then % inhibition of cytokine (depicted by the color scale provided) was determined for individual mice from the Fc control, abatacept, or acazicolcept-treated ("Exp") groups relative to DPBS mice using the following formula: ((Avg DPBS – Exp Animal)/Avg DPBS))*100. The study was repeated twice with similar trends observed for efficacy of acazicolcept.

Histological analysis

Mice were sacrificed after clinical scoring on day 34. Paws were collected in formalin, decalcified, sectioned, and stained with toluidine blue. Paw histology scores were determined using a scoring system that considered joint inflammation, pannus formation, cartilage damage, and bone resorption, with a score of 0–5 (ranging from none to severe) for each parameter. Histological analysis was performed on all samples by a pathologist, blind to treatment conditions and clinical scores.

Flow cytometric analysis of popliteal lymph nodes

Popliteal lymph nodes (LN) from the hind legs were collected from representative mice in each group (i.e., with disease activity scores clustered around the group mean paw score) for evaluation by flow cytometry. Single cell suspensions were prepared by teasing LNs apart with forceps and passing over a nylon filter to remove debris. For flow cytometric analysis, $0.5 – 1 \times 10^6$ live LN cells from individual mice were stained with viability stains (Near Infra-Red at a 1:1000 dilution or Blue at a 1:1500 dilution; ThermoFisher,) according to the manufacturer's instructions, followed by resuspension of the cell pellets in 5 μg/mL mouse Fc block/anti-CD16/32 (clone 93; BioLegend) and a 45-min incubation on ice with a cocktail including fluorescently-labeled anti-mouse antibodies against CD19 (1:100 dilution, clone 1D3; Beckton Dickinson), CD4 (1:100 dilution, clone GK1.5; Beckton Dickinson), CD8 (1:100 dilution, clone 53-6.7; BioLegend), GL7 (1:100 dilution, clone GL7; BioLegend), CXCR5 (1:100 dilution, clone L138D7; BioLegend), and PD-1 (1:100 dilution, clone 29F.1A12; BioLegend). For intracellular cytokine staining, separate wells of LN cells were stimulated for 6 hours with PMA/ionomycin + Golgi Plug and Golgi Stop (37°C) (Becton Dickinson), then fixed and permeabilized prior to a 45-min incubation at 25°C with anti-mouse IL-17A (1:20 dilution; clone TC11-18H10.1; BioLegend) or anti-mouse IFNγ (1:20 dilution; clone XMG1.2; BioLegend). Surface-stained unstimulated, fixed/permeabilized LN cells were included as controls. Stained samples were washed and collected on a Becton Dickinson LSRII flow cytometer. Cell subsets were identified and quantified using FlowJo v10 software.

Statistical analysis

In the CIA model, significant differences between groups were analyzed using the following tests: 2-way repeated-measures ANOVA (for 'treatment' effect) for body weight and paw scores over time; Kruskal-Wallis test with Dunn's multiple comparisons test for anti-collagen antibodies, paw histology scores, and final paw scores at termination; 1-way ANOVA with Tukey's multiple comparisons test for lymph node flow cytometry; unpaired 2-tailed Student's t-test for serum cytokine data. Estimation plots were prepared using GraphPad Prism® software (Version 9.0.2), which was also used for statistical analyses; *p*-values <0.05 were considered statistically significant for all statistical tests.

Human PBMC stimulation and cytokine assays

PBMC from RA or PsA patients (BioIVT, Westbury, NY) and healthy donors (Bloodworks Northwest; Seattle, WA) were stimulated with aAPC (K562/OKT3/CD80/CD86/ICOSL) for 48 hours in the presence of 100 nM Fc for test articles or 100 nM each for the abatacept and prezalumab combination. Note that 100 nM acazicolcept or abatacept is sufficient to block CD80 or CD86 ligand binding to CD28 and 100 nM acazicolcept or prezalumab is sufficient to block ICOSL binding to ICOS, as assessed via flow cytometry. Supernatants were collected and assayed for GM-CSF, IFNγ, IL-12p70, IL-13, IL-17A, IL-17F, IL-2, IL-21, IL-6, and TNFα by ELISA or Luminex multiplex (Millipore). Percent inhibition was determined using the following formula: ((Fc control value – Experimental value)/Fc control value))*100.

Gene expression analysis

Total RNA (0.5 ng) was added to lysis buffer from the SMART-Seq v4 Ultra Low Input RNA Kit for Sequencing (Takara) and subjected to RT-PCR to generate full-length amplified cDNA. Sequencing libraries were constructed using the NexteraXT DNA sample preparation kit (Illumina) to generate Illumina-compatible barcoded libraries. Libraries were pooled and quantified using a Qubit® Fluorometer (Life Technologies). Dual-index, single-read sequencing of pooled libraries was carried out on a HiSeq2500 sequencer (Illumina) with 58-base reads, using HiSeq v4 Cluster and SBS kits (Illumina) with a target depth of 5 million reads per sample. Base calls were processed to FASTQs on BaseSpace (Illumina), and a base call quality-trimming step was applied to remove low-confidence base calls from the ends of reads. The FASTQs were aligned to the GRCh38 reference genome using STAR v.2.4.2a, and gene counts were generated using htseq-count. QC and metrics analysis was performed using the Picard family of tools (v1.134). Transcripts per million (TPM) values were calculated using the gene lengths from GRCh38, as downloaded via BioMart (ensembl.org) using the May 2012 version. The raw counts for each gene were divided by the length of the gene and multiplied by 1000, then all the values were divided by the number of million reads in that sample. Differential expression analysis was performed using the DESeq2 R package (v1.34.0). Genes with Benjamini-Hochberg (BH) adjusted p value of <0.05, and a fold change with absolute value

>1.5 were considered significant. For pathway analysis, significant genes were input into Ingenuity Pathway Analysis (IPA, v22.0.2; Qiagen).

Supplementary Table 1: PBMC Donor Demographics and Disease Status at Time of Collection

Healthy Donors				
Age (yr)	**Sex**	**Race**		
39	M	Hispanic		
27	M	Not reported		
53	M	Caucasian		
49	F	Multiracial		
50	F	Caucasian		
35	F	Caucasian		
57	M	Caucasian		
56	M	African American		
39	M	Hispanic		
Unknown	Unknown	Unknown		
Rheumatoid Arthritis				
Age (yr)	**Sex**	**Race**	**Anti-CCP/RF**	**CRP/ESR**
65	F	Caucasian	60/89	10.5/14
59	F	Hispanic	>250/83	0.1/1
61	F	Caucasian	>250/192	1.0/16
89	F	Caucasian	0/21	4.2/9
56	M	Caucasian	>250/494	5.5/16
77	F	Hispanic	61/257	51/40
38	F	Hispanic	250/21	0.8/2
32	F	Caucasian	>250/21	0.2/30
45	F	Caucasian	>250/21	2.7/6
30	F	African American	>250/281	1.2/33
70	F	Caucasian	>250/34.8	1.8/9
84	M	Caucasian	>250/110	5.9/2
72	F	Caucasian	>250/69.3	0.1/2
46	F	Hispanic	<16/12	2.1/6
83	F	Caucasian	16/9	5.3/19

Psoriatic Arthritis					
Age (yr)	**Sex**	**Race**	**TJC/SJC**	**CRP/ESR**	**PASI**
51	M	Hispanic	6/4	0.38/7	20.4
73	F	Caucasian	12/10	13.5/60	1
63	F	Caucasian	21/Unknown	0.8/2	0
61	F	African American	4/4	5.9/36	1
39	M	Hispanic	Unknown/ Unknown	59.6/39	Unknown
50	M	Caucasian	8/8	4.3/2	14.1
60	F	Caucasian	42/42	2.0/2.2	3.4
53	F	African American	37/19	3.3/37	0.6
60	F	Caucasian	4/0	3.5/31	0
64	F	Caucasian	24/10	15.7/40	0.7
58	F	Caucasian	0/2	4.7/5	2.4
43	F	Caucasian	42/21	10.8/1	0.2
47	M	Hispanic	3/0	1.94/6	9.6
55	F	American Indian	4/0	0.4/2	6.3
60	M	Caucasian	2/0	1.5/9	0.9

CCP = cyclic citrullinated peptide; RF = rheumatoid factor; CRP/ESR = C-reactive protein/ erythrocyte sedimentation rate; TJC/SJC = tender joint count/swollen joint count; PASI = Psoriasis area and severity index

Supplementary Figure Legends

Supplementary Figure 1. **Acazicolcept is more effective than abatacept at reducing terminal paw and histological scores in the mouse CIA model.**

A. Design of the mouse CIA study using a semi-therapeutic dosing regimen, with test article administration initiated on Study Day 18 together with the collagen boost. **B**. Final CIA paw scores on Day 34; horizontal lines and error bars depict

the median ± interquartile ranges for each group (* p<0.05, **** p<0.0001 by Kruskal-Wallis test and Dunn's multiple comparisons test). **C**. Stained sections of each paw were analyzed and scored using the scoring system described in Methods. Paw scores (median ± interquartile ranges) for each individual parameter are shown for each treatment group (* p<0.05, **** p<0.0001 by Kruskal-Wallis test and Dunn's multiple comparisons test).

Supplementary Figure 2. Acazicolcept significantly downregulates more key genes associated with RA and PsA disease pathogenesis relative to single pathway inhibitors alone or in combination

RNA was isolated from cells harvested from the PBMC/aAPC co-cultures described in Figure 3 and subjected to RNASeq analysis, as described in Materials and Methods. The number of transcripts per million (TPM) for key inflammatory genes *IL17A*, *IL17F*, *TNF*, *IFNG*, and *IL6* were plotted for PBMC/aAPC co-culture samples collected from **A.** RA patients and **B.** PsA patients. Estimation plots are provided for each gene, comparing acazicolcept-containing cultures to those containing abatacept+prezalumab. More genes significantly associated with disease pathogenesis were significantly downregulated by acazicolcept than by abatacept alone or in combination with prezalumab. Criteria for genes reduced by acazicolcept: false discovery rate (FDR)<0.05, LogFC<-0.5. Full lists of genes that were downregulated by acazicolcept and comparator treatments are provided in Supplementary Information.

Supplementary Figure 3. Acazicolcept inhibits upregulation of *ICOS* and *PDCD1* (PD-1) gene expression, but does not significantly affect CD28 transcript levels

RNA was isolated from cells harvested from the PBMC/aAPC co-cultures described in Figure 3 and subjected to RNASeq analysis, as described in Materials and Methods. The number of transcripts per million (TPM) for *ICOS*, *PDCD1*, and *CD28* were plotted for PBMC/aAPC co-culture samples collected from **A.** RA patients and **B.** PsA patients. Estimation plots are provided for each gene, comparing acazicolcept-containing cultures to those containing abatacept+prezalumab. Criteria for genes reduced by acazicolcept: false discovery rate (FDR)<0.05, LogFC<-0.5.

Supplementary Figure 4. PBMC from PsA patients have a transcriptional signature distinct from the other PBMC types in the absence of aAPC stimulation.

RNA was isolated from cells harvested from control unstimulated and untreated HD, RA, and PsA PBMC cultures, included in the experiments described in Figure 3, and subjected to RNASeq analysis as described in Materials and Methods. **A.** Vst-transformed raw gene counts were plotted using PCA analysis for unstimulated/untreated HD, RA, and PsA patient PBMCs. Differentially expressed genes in unstimulated HD vs RA **B.** or HD vs PsA **C.** PBMC cultures. **B.-C.** Volcano plots where differentially expressed genes with a BH-adjusted *p*-value <0.05 (horizontal dashed line) and absolute value fold change >1.5 (vertical

dashed line) were considered significant (yellow dots). **D.-E.** Transcripts per million were plotted for indicated genes with all treatment groups compared to Fc control within each respective donor/disease type (HD, RA, PsA). (*p<0.05, **p<0.01, ***p<0.001, ****p<0.0001 by two-way ANOVA). **F.** Differentially expressed genes from Figure **5B** were input into Ingenuity Pathway Analysis to identify canonical pathways that were upregulated with acazicolcept treatment relative to abatacept+prezalumab. Pathways with IPA z-score >2 and BH adjusted p-value <0.1 were considered significant.

Acazicolcept, a Dual ICOS/CD28 Antagonist, Reveals Nonredundant Roles of T Cell Costimulation Pathways in Inflammatory Arthritis

Acazicolcept is more effective than abatacept in a mouse collagen-induced arthritis model

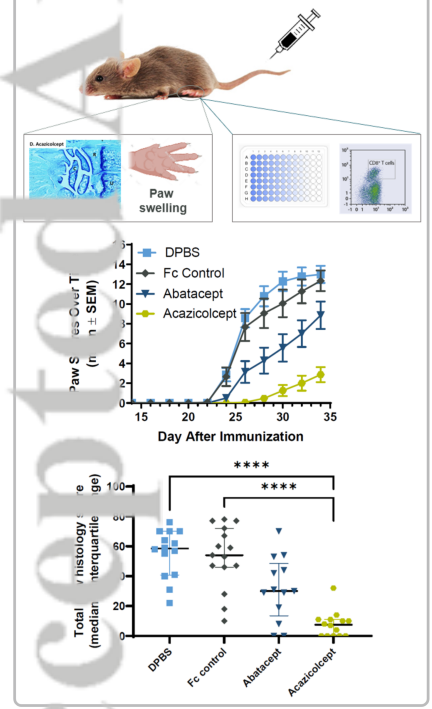

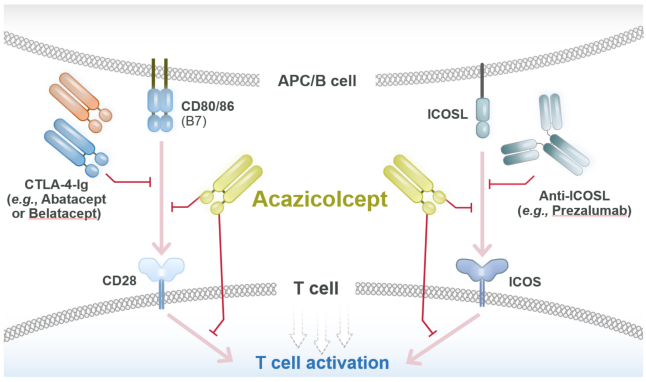

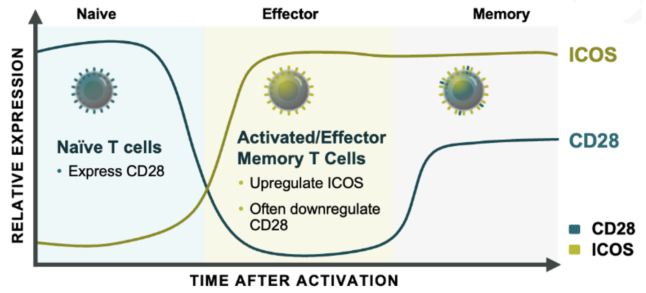

ARTHRITIS MAY REQUIRE TARGETING BOTH:

- **CD28:** new / naïve T cells
- **ICOS:** activated T cells

Acazicolcept suppresses T cell activation more potently than abatacept and prezalumab combined

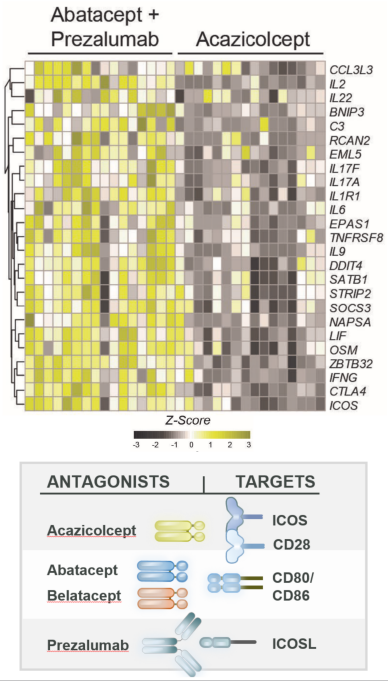

Dillon SR, Evans LS, Lewis KE, et al. Dual Blockade of ICOS and CD28 with acazicolcept (ALPN-101) reveals nonredundant roles of T cell costimulation pathways in inflammatory arthritis. Arthritis Rheumatol 2023.

Arthritis & Rheumatology ACR American College of Rheumatology

ART_42484_Dillon_GraphicalAbstract_ar-22-0762.R1.png

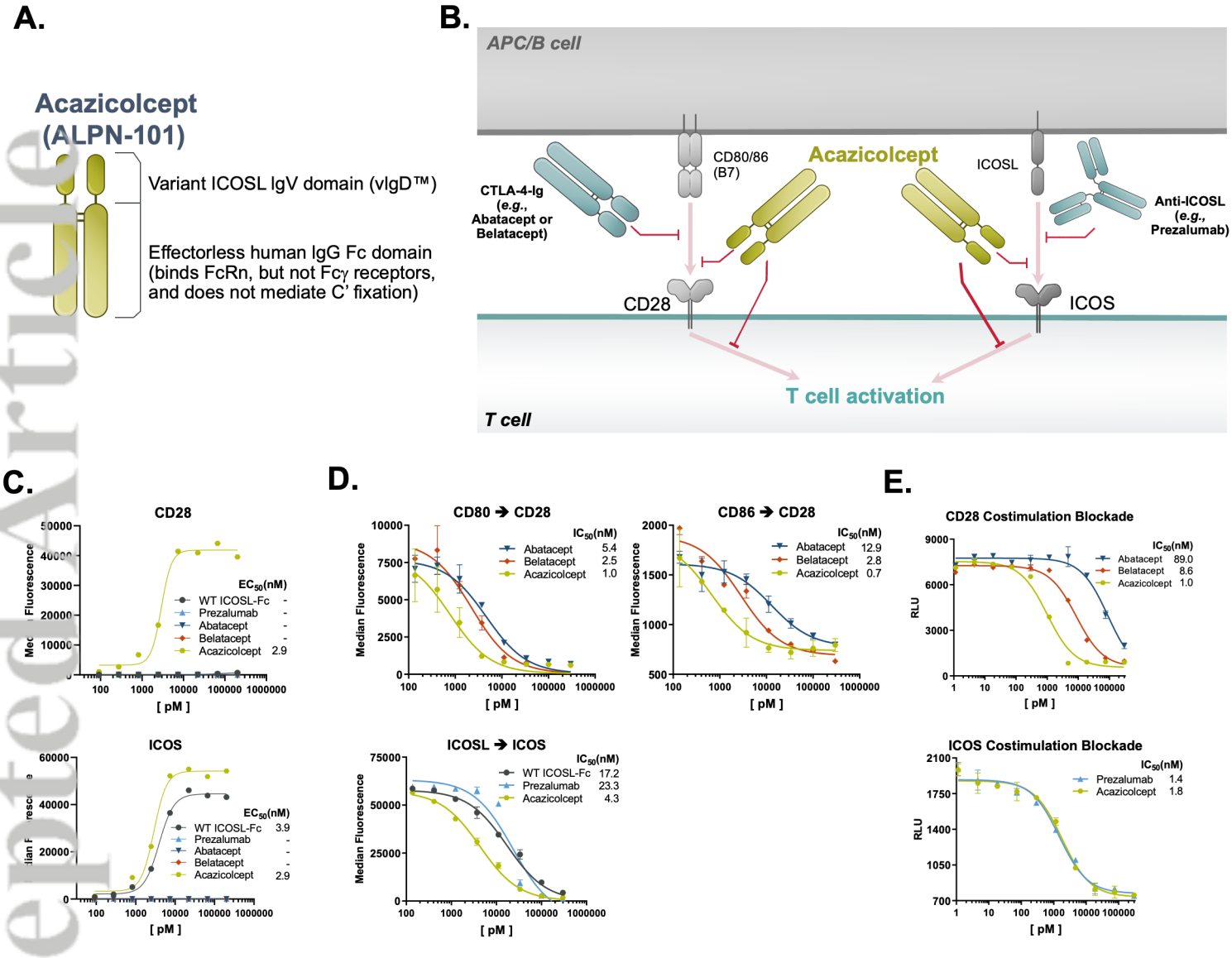

ART_42484_Fig 1.tif

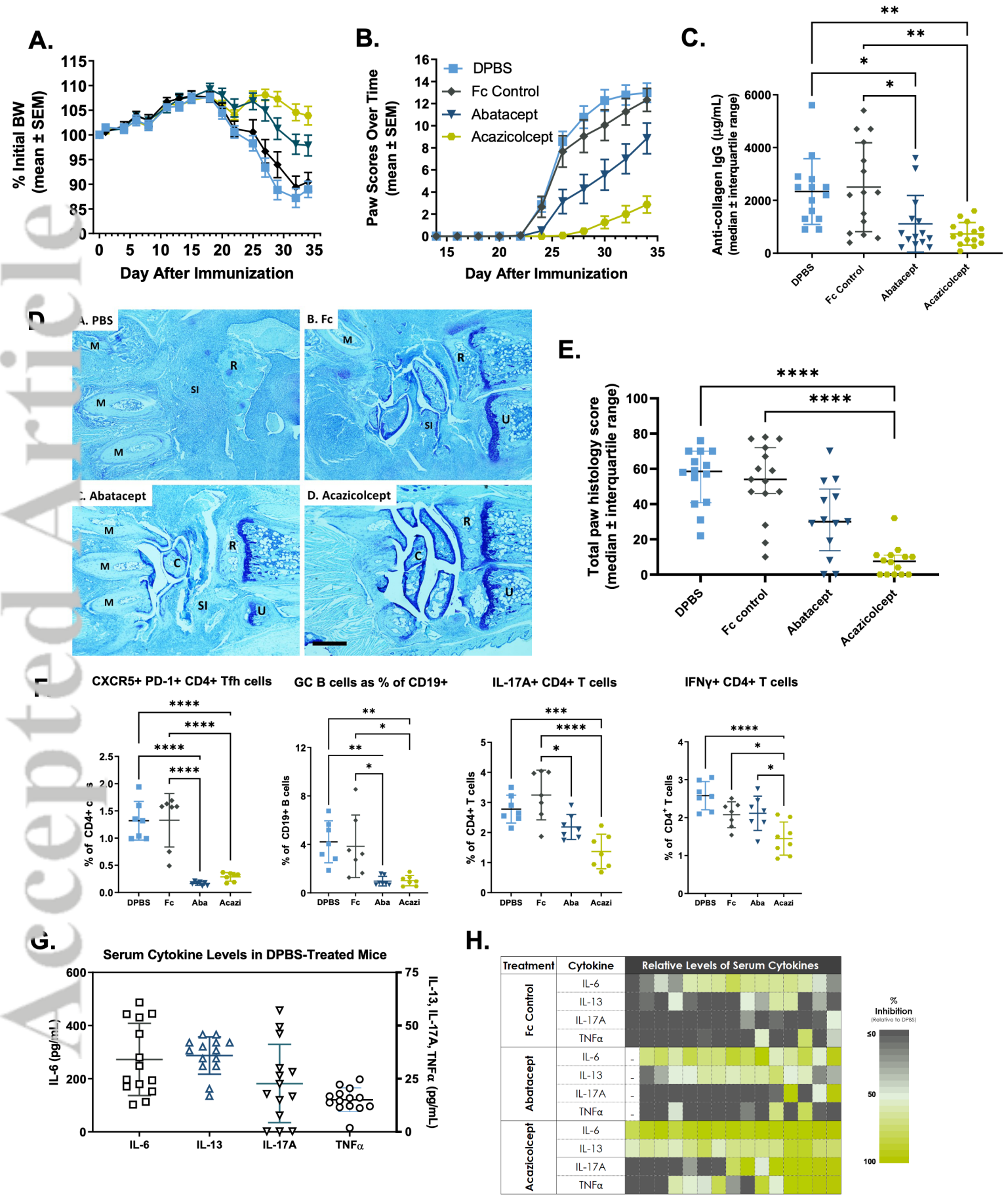

ART_42484_Fig 2.tif

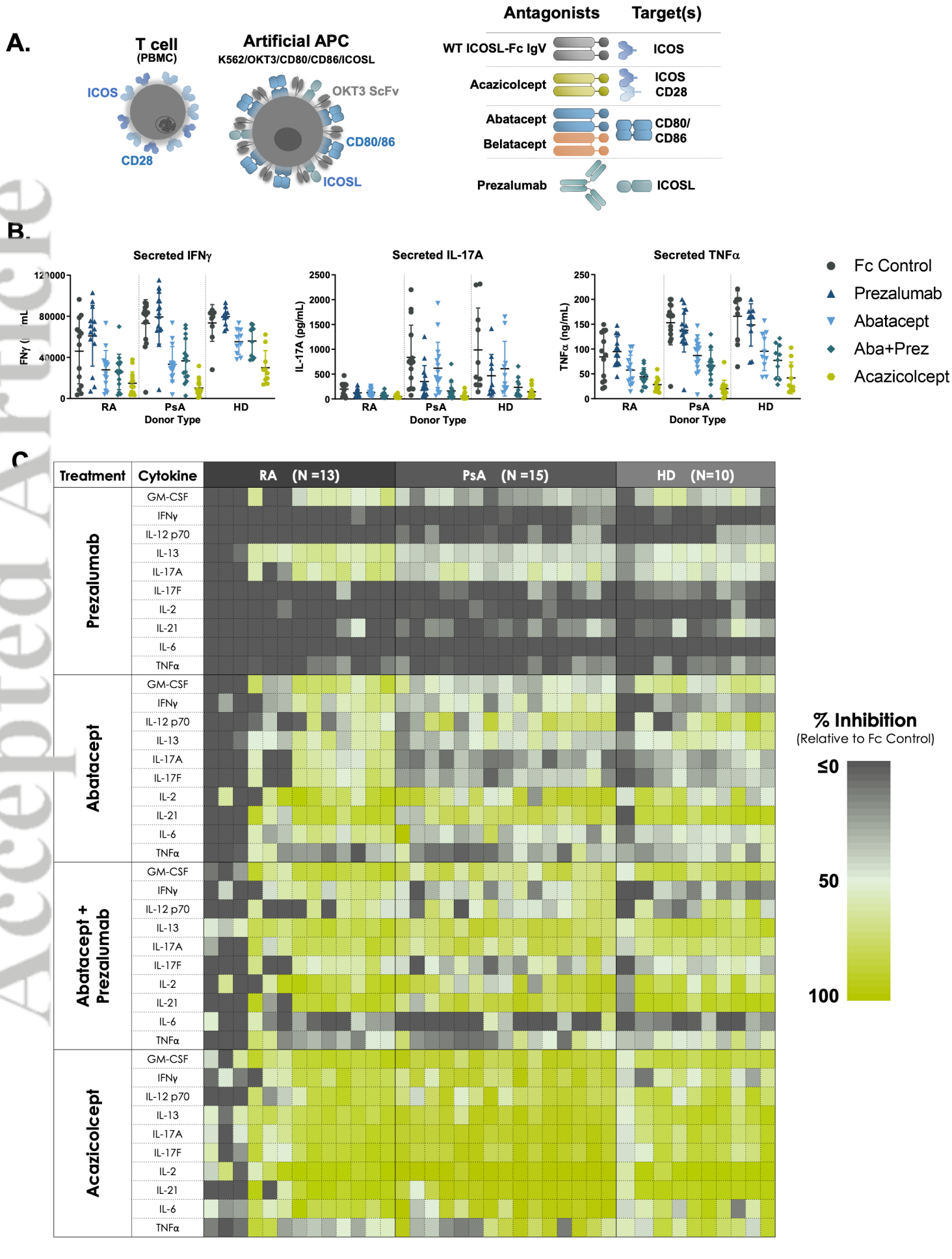

ART_42484_Fig 3.tif

A.

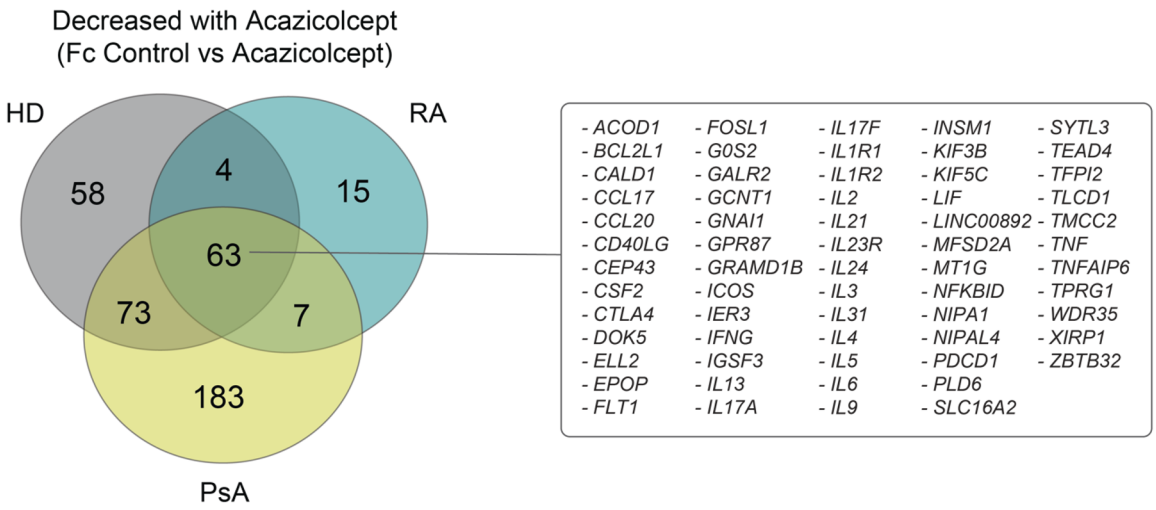

B.

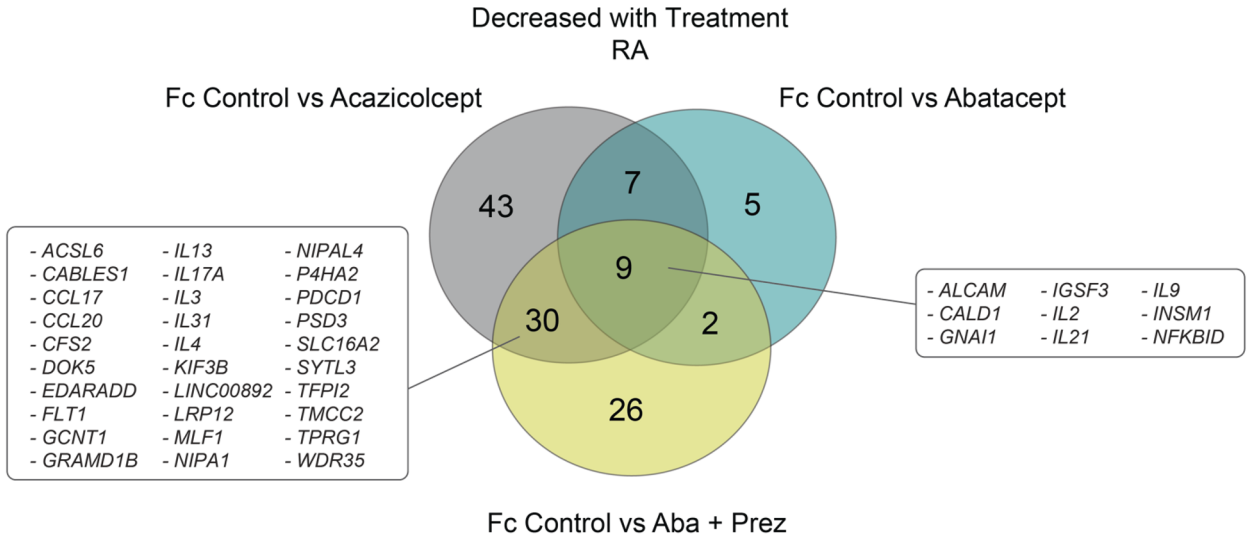

C.

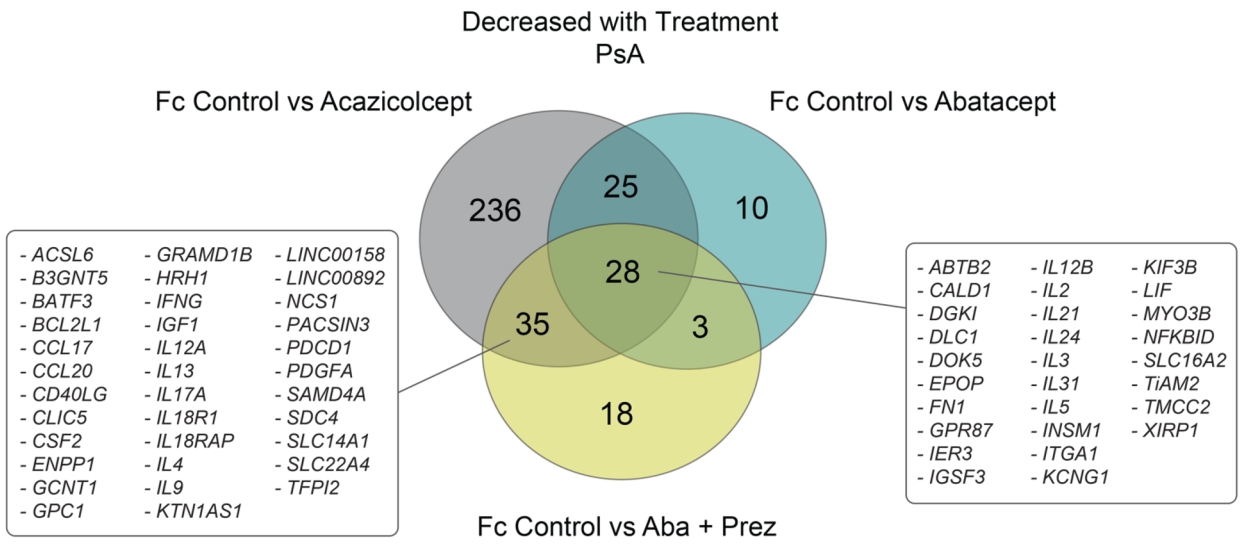

ART_42484_Fig 4.tif

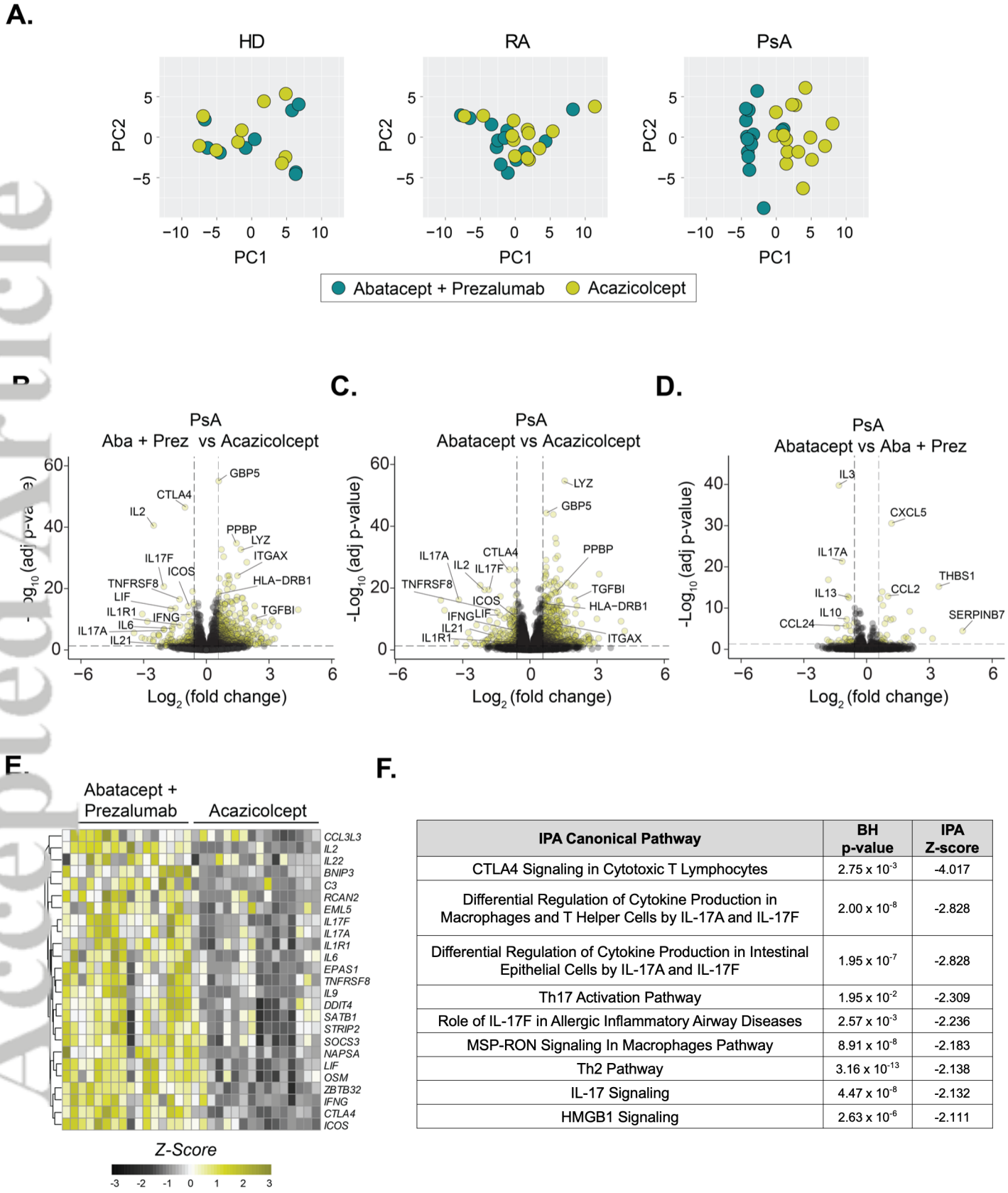

IPA Canonical Pathway	BH p-value	IPA Z-score
CTLA4 Signaling in Cytotoxic T Lymphocytes	2.75×10^{-3}	-4.017
Differential Regulation of Cytokine Production in Macrophages and T Helper Cells by IL-17A and IL-17F	2.00×10^{-8}	-2.828
Differential Regulation of Cytokine Production in Intestinal Epithelial Cells by IL-17A and IL-17F	1.95×10^{-7}	-2.828
Th17 Activation Pathway	1.95×10^{-2}	-2.309
Role of IL-17F in Allergic Inflammatory Airway Diseases	2.57×10^{-3}	-2.236
MSP-RON Signaling In Macrophages Pathway	8.91×10^{-8}	-2.183
Th2 Pathway	3.16×10^{-13}	-2.138
IL-17 Signaling	4.47×10^{-8}	-2.132
HMGB1 Signaling	2.63×10^{-6}	-2.111